Journal of Physical Chemistry & Biophysics

Fouda et al. J Physic Chem Biophysic 2011, S:4
DOI: 10.4172/2161-0398.S4-001

Research Article Open Access

Helicity and Wave Switching in a Nonlinear Model of DNA Dynamics

H. P. Ekobena Fouda[1], C. B. Tabi[1,2]*, S. Zdravkovic[2,3] and T. C. Kofane[4]

[1]Laboratory of Biophysics, Department of Physics, Faculty of Science, University of Yaounde I, P.O. Box 812, Yaounde, Cameroon
[2]The Abdus Salam International Centre for Theoretical Physics, Trieste, Italy
[3]Fakultet tehnickih nauka, Univerzitet u Pristini, Kosovska Mitrovica, Serbia
[4]Laboratory of Mechanics, Department of Physics, Faculty of Science, University of Yaounde I, P.O. Box 812, Yaoune, Cameroon

Abstract

We have introduced helicity in the revised Hamiltonian in which the dipole-dipole interaction and dipoleinduced-dipole interaction have taken into account. The system has been shown to be govern by a set of coupled discrete sine-Gordon equations, which describe the bending and oscillations of the hydrogen bonds. The multiple scale expansion has been used and the stability of planar waves, solutions of the system, has been investigated. We have brought out the effect of discreteness and have shown that helicity brings about wave switching in the two-component DNA model under study.

PACS number(s): 87.14.gk, 05.45.Yv, 87.15.H.

Keywords: DNA dynamics; Helicity; Modulational instability; Soliton

Introduction

The complexity and role of DNA make it the most important molecule in nature. Describing its dynamics therefore remains a fascinated task for modern physicists and biophysicists alike, because it is nowadays accepted that DNA undergoes dynamical features that are not yet fully unmasked. There have been many attempts to describe that complicated dynamics using appropriate models. The first nonlinear model was suggested by Englander et al. [1]. Later, Yomosa proposed a further theory based on a dynamic plane base-rotor model [2]. Along the same line, Takeno and Homma [3] developed that idea and proposed a general spin-like model, and showed its efficiency in describing open-states in DNA. Further modifications of the Yomosa's model have been introduced by Zhang [4] to show the influence of the dipole-dipole energy on the soliton excitations in the B-DNA molecule. He therefore proposed the Hamiltonian

$$H_0 = \sum_n \left[\frac{1}{2} I\left(\dot{\psi}_n^2 + \dot{\psi}_n'^2\right) + \frac{1}{2} S\left(\psi_{n+1} - \psi_n\right)^2 + \frac{1}{2} S\left(\psi'_{n+1} - \psi'_n\right)^2 + V\left(\psi_n, \psi'_n\right) \right], \quad (1)$$

Where I is the mean value of the moment of inertia of the bases for the rotation around the axes P and P' which pass through the point P^n and P'_n and are in parallel with z axis, respectively, S is a parameter associated with the stacking energy. $V\left(\psi_n, \psi'_n\right)$ is the interstrand interaction energy which describes interactions between hydrogen bonds. It is given by

$$V\left(\psi_n, \psi'_n\right) = D\left[1 - \cos\left(\psi_n - \psi'_n\right)\right] + \lambda\left(2 - \cos\psi_n - \cos\psi'_n\right) + \beta\left\{3\left(1 - \cos\psi_n \cos\psi'_n\right) - \left[1 - \cos\left(\psi_n - \psi'_n\right)\right]\right\} \quad (2)$$

The first term of Eq. (2) is the usual interstrand potential, where D is a parameter associated with the hydrogen bond energy. The second term describes the dipole-induced-dipole interaction between two bases of the nth base pair, with λ being a coupling constant associated with the dipole-induced-dipole interaction energy. The last term describes the dipole-dipole interactions between two bases in the nth coplanar base pair, where β measures the strength of the dipole-dipole interactions between hydrogen bonds.

As described above, one sees that the model does not take helicity into account. It is the main purpose of the present work to modify the above-presented model and show, through the stability analysis of a plane wave, that helicity can bring about interesting features in the dynamics of DNA molecules. In fact, helicity has already been introduced in some recent models by many authors [5-7]. It has been, for example, pointed out that it can bring about highly localized structures and even describe open-states in DNA in a more realistic way [5,6,9,10].

Helicity is due to water filaments that link units at different sites. In particular, they have a good probability to form between nucleotides which are a half turn of the helix apart on different chains, i.e., which are near to each other in space due to the double helix geometry; these water filaments-mediated interactions are therefore also called helicoidal interactions (the nth pair interact with both the $(n + h)$th and $(n – h)$th pairs) [5,6,8] with a pitch h that could be equal to 4 [8,9] or to 5 [5,10]. Since the helicoidal pitch is 11, we will use in the rest of the paper $h = 5$. Helicoidal interactions are usually described by the potential

$$H_1 = \sum_n \frac{1}{2} S_h \left[\left(\psi_{n+h} - \psi'_n\right)^2 + \left(\psi'_{n+h} - \psi_n\right)^2 \right], \quad (3)$$

Where S_h is a parameter associated with the helicoidal interaction energy. Taking account of Eq. (2) and (3), the dynamics of the molecules is described by the set of coupled equations

$$I\ddot{\varphi}_n = -3\beta \sin\varphi_n - 2\lambda \sin\frac{\varphi_n}{2}\cos\frac{\phi_n}{2} + S\left(\varphi_{n-1} - 2\varphi_n + \varphi_{n+1}\right) + S_h\left(\varphi_{n-h} - 2\varphi_n + \varphi_{n+h}\right) \quad (4a)$$

$$I\ddot{\phi}_n = -\left(2D + \beta\right)\sin\phi_n - 2\lambda \sin\frac{\phi_n}{2}\cos\frac{\varphi_n}{2} + S\left(\phi_{n-1} - 2\phi_n + \phi_{n+1}\right) - S_h\left(\phi_{n-h} + 2\phi_n + \phi_{n+h}\right), \quad (4b)$$

***Corresponding author:** C. B. Tabi, The Abdus Salam International Centre for Theoretical Physics, Trieste, Italy, E-mail: contab408@hotmail.com

Received November 07, 2011; **Accepted** January 23, 2012; **Published** January 26, 2012

Citation: Fouda HPE, Tabi CB, Zdravkovic S, Kofane TC (2012) Helicity and Wave Switching in a Nonlinear Model of DNA Dynamics. J Physic Chem Biophysic S4:001. doi:10.4172/2161-0398.S4-001

Where $\varphi = \psi + \psi'$ and $\phi = \psi - \psi'$. By letting S_h=0 we recover the system as described by Zhang [4]. Furthermore, works on that model has considered the continuum approximation of the above equations. In recent works, discreteness effects have been shown to fully modify the analytical treatment of DNA model [11-13]. In that respect, in order to avoid dropping important information about the model, we adopt a purely discrete approach and show that the model can be reduced to a set of coupled modified nonlinear Schrodinger equations. In this frame, we apply the multiple-scale expansion introduced by Leon and Manna [14,15] and successfully applied by us in recent papers [5,16]. The procedure is fully explained in [14,15] and [5,16], but, to our knowledge, it has never been applied to the above coupled discrete systems. In a recent work [5], the above equations have been shown to be completely decoupled. In the present case they constitute a coupled system which describes acoustical and optical waves that propagate in the molecule. It is therefore likely that the group velocities and frequencies are not the same. This makes the problem to solve rather complicated. For instance, by means of the change in independent variables $\tau_1 = \varepsilon\left(t + nd/\upsilon_{g1}\right)$, $\tau_2 = \varepsilon\left(t + nd/\upsilon_{g2}\right)$ and $\varsigma = \varepsilon^2 n$ it is possible to use the trial solutions [5,14-16]

$$\varphi_n(t) = \sum_{p=1}^{\infty}\sum_{l=-p}^{p} \varepsilon^p \chi_p^{(l)}(m,\tau_1) A_1^{(l)}(n,t) \tag{5}$$

$$\phi_n(t) = \sum_{p=1}^{\infty}\sum_{l=-p}^{p} \varepsilon^p \eta_p^{(l)}(m,\tau_2) A_2^{(l)}(n,t), \tag{6}$$

With $A_j^{(l)}(n,t) = \exp\left(il\left(\Omega_j t + qdn\right)\right)(j=1,2), \eta_p^{(-l)} = \left(\eta_p^{(l)}\right)^*$, and $\chi_p^{(-l)} = \left(\chi_p^{(l)}\right)^* \cdot \upsilon_{gj}$ and Ω_j are the group velocities and the frequencies of both modes, respectively.

We insert the above set of solutions into Eqs. (4) and we get the following system

$$\begin{aligned}
&\sum_{p=1}^{\infty}\varepsilon^p\sum_{l=-p}^{p}\left\{I\left[\varepsilon^2\partial_{\tau_1\tau_1}\chi_p^{(l)}(m,\tau_1) + 2i\varepsilon l\Omega_1\partial_{\tau_1}\chi_p^{(l)}(m,\tau_1) - \left(l\Omega_1\right)^2\chi_p^{(l)}(m,\tau_1)\right]\right.\\
&-S\left[\left(e^{ilqd}+e^{-ilqd}-2\right)\chi_p^{(l)}(m,\tau_1) + \varepsilon\left(\frac{d}{\upsilon_{g1}}\right)\left(e^{ilqd}-e^{-ilqd}\right)\partial_{\tau_1}\chi_p^{(l)}(m,\tau_1)\right.\\
&\left.+\frac{\varepsilon^2}{2}\left(e^{ilqd}+e^{-ilqd}\right)\left(\frac{d}{\upsilon_{g1}}\right)\partial_{\tau_1\tau_1}\chi_p^{(l)}(m,\tau_1) + \frac{\varepsilon^2}{2}\left(e^{ilqd}-e^{-ilqd}\right)\left(\chi_p^{(l)}(m+1,\tau_1) - \chi_p^{(l)}(m-1,\tau_1)\right)\right]\\
&+S_h\left[\left(e^{ilqd}+e^{-ilqd}-2\right)\chi_p^{(l)}(m,\tau_1) + \varepsilon\left(\frac{hd}{\upsilon_{g1}}\right)\left(e^{ilqd}-e^{-ilqd}\right)\partial_{\tau_1}\chi_p^{(l)}(m,\tau_1)\right.\\
&\left.+\frac{\varepsilon^2}{2}\left(e^{ilqd}+e^{-ilqd}\right)\left(\frac{hd}{\upsilon_{g1}}\right)\partial_{\tau_1\tau_1}\chi_p^{(l)}(m,\tau_1) + \frac{\varepsilon^2}{2}\left(e^{ilqd}-e^{-ilqd}\right)\left(\chi_p^{(l)}(m+h,\tau_1) - \chi_p^{(l)}(m-h,\tau_1)\right)\right]\\
&\left.+\left(\beta+\lambda\right)\left[\chi_p^{(l)}(m,\tau_2)A_1^{(l)}(n,t)\right]\right\}A_1^{(l)}(n,t) - \left(\frac{\beta}{2}+\frac{\lambda}{24}\right)\left[\sum_{p=1}^{\infty}\varepsilon^p\sum_{l=-p}^{p}\chi_p^{(l)}(m,\tau_1)A_1^{(l)}(n,t)\right]^3\\
&-\frac{\lambda}{8}\left[\sum_{p=1}^{\infty}\varepsilon^p\sum_{l=-p}^{p}\eta_p^{(l)}(m,\tau_2)A_2^{(l)}(n,t)\right]^2\left[\sum_{p=1}^{\infty}\varepsilon^p\sum_{l=-p}^{p}\chi_p^{(l)}(m,\tau_1)A_1^{(l)}(n,t)\right] = 0
\end{aligned} \tag{7a}$$

$$\begin{aligned}
&\sum_{p=1}^{\infty}\varepsilon^p\sum_{l=-p}^{p}\left\{I\left[\varepsilon^2\partial_{\tau_2\tau_2}\eta_p^{(l)}(m,\tau_2) + 2i\varepsilon l\Omega_2\partial_{\tau_2}\eta_p^{(l)}(m,\tau_2) - \left(l\Omega_2\right)^2\chi_p^{(l)}(m,\tau_2)\right]\right.\\
&-S\left[\left(e^{ilqd}+e^{-ilqd}-2\right)\eta_p^{(l)}(m,\tau_2) + \varepsilon\left(\frac{d}{\upsilon_{g2}}\right)\left(e^{ilqd}-e^{-ilqd}\right)\partial_{\tau_2}\chi_p^{(l)}(m,\tau_2)\right.\\
&\left.+\frac{\varepsilon^2}{2}\left(e^{ilqd}+e^{-ilqd}\right)\left(\frac{d}{\upsilon_{g2}}\right)\partial_{\tau_2\tau_2}\eta_p^{(l)}(m,\tau_2) + \frac{\varepsilon^2}{2}\left(e^{ilqd}-e^{-ilqd}\right)\left(\eta_p^{(l)}(m+1,\tau_2) - \eta_p^{(l)}(m-1,\tau_2)\right)\right]\\
&+S_h\left[\left(e^{ilqd}+e^{-ilqd}-2\right)\eta_p^{(l)}(m,\tau_2) + \varepsilon\left(\frac{hd}{\upsilon_{g2}}\right)\left(e^{ilqd}-e^{-ilqd}\right)\partial_{\tau_2}\chi_p^{(l)}(m,\tau_2)\right.\\
&\left.+\frac{\varepsilon^2}{2}\left(e^{ilqd}+e^{-ilqd}\right)\left(\frac{hd}{\upsilon_{g2}}\right)\partial_{\tau_2\tau_2}\eta_p^{(l)}(m,\tau_2) + \frac{\varepsilon^2}{2}\left(e^{ilqd}-e^{-ilqd}\right)\left(\eta_p^{(l)}(m+h,\tau_2) - \eta_p^{(l)}(m-h,\tau_2)\right)\right]\\
&\left.+\left(2\beta+D+\lambda\right)\left[\eta_p^{(l)}(m,\tau_2)A_2^{(l)}(n,t)\right]\right\}A_2^{(l)}(n,t) - \left(\frac{\beta}{3}+\frac{D}{6}+\frac{\lambda}{24}\right)\left[\sum_{p=1}^{\infty}\varepsilon^p\sum_{l=-p}^{p}\eta_p^{(l)}(m,\tau_2)A_2^{(l)}(n,t)\right]^3\\
&-\frac{\lambda}{8}\left[\sum_{p=1}^{\infty}\varepsilon^p\sum_{l=-p}^{p}\eta_p^{(l)}(m,\tau_1)A_1^{(l)}(n,t)\right]^2\left[\sum_{p=1}^{\infty}\varepsilon^p\sum_{l=-p}^{p}\chi_p^{(l)}(m,\tau_2)A_1^{(l)}(n,t)\right] = 0
\end{aligned} \tag{7b}$$

We solve the problem for different orders of the parameter ε. In this frame, the coefficients for constant terms give at different orders of ε

$$\varepsilon:\eta_1^{(0)}=\chi_1^{(0)}=0\,;\varepsilon^2:\eta_2^{(0)}=\chi_2^{(0)}=0\,;\ \varepsilon^3:\eta_3^{(0)}=\chi_3^{(0)}=0 \tag{8}$$

The coefficients of $A_j^{(1)}(j=1,2)$, at different order of ε, give

$$\varepsilon^1:\Omega_1^2=\frac{1}{I}\left[(\beta+\lambda)+4S\sin^2\left(\frac{qd}{2}\right)+4S_h\sin^2\left(\frac{hqd}{2}\right)\right],$$

$$\Omega_2^2=\frac{1}{I}\left[(2\beta+D+\lambda)+4S\sin^2\left(\frac{qd}{2}\right)+4S_h\cos^2\left(\frac{hqd}{2}\right)\right]$$

$$\varepsilon^2:\upsilon_{g1}=\frac{d\left[S\sin(qd)+hS_h\sin(hqd)\right]}{I\Omega_1},\upsilon_{g2}=\frac{d\left[S\sin(qd)+hS_h\sin(hqd)\right]}{I\Omega_2}$$

$$\varepsilon^3:\left[I-S\left(\frac{d}{\upsilon_{g1}}\right)^2\cos(qd)-S_h\left(\frac{hd}{\upsilon_{g1}}\right)^2\cos(hqd)\right]\frac{\partial^2\chi_1^{(1)}}{\partial\tau_1^2}-iS\sin(qd)\left[\chi_1^{(1)}(m-1)\right]$$

$$-iS_h\sin(hqd)\left[\chi_1^{(1)}(m+h)-\chi_1^{(1)}(m-h)\right]-\left[3\left(\frac{\beta}{2}+\frac{\lambda}{24}\right)\left|\chi_1^{(1)}\right|^2+\frac{\lambda}{4}\left|\eta_1^{(1)}\right|^2\right]\chi_1^{(1)}=0$$

$$\left[I-S\left(\frac{d}{\upsilon_{g2}}\right)^2\cos(qd)+S_h\left(\frac{hd}{\upsilon_{g2}}\right)^2\cos(hqd)\right]\frac{\partial^2\eta_1^{(1)}}{\partial\tau_2^2}-iS\sin(qd)\left[\eta_1^{(1)}(m+1)-\eta_1^{(1)}(m-1)\right]$$

$$+iS_h\sin(hqd)\left[\eta_1^{(1)}(m+h)-\eta_1^{(1)}(m-h)\right]-\left[3\left(\frac{\beta}{3}+\frac{D}{6}+\frac{\lambda}{24}\right)\left|\eta_1^{(1)}\right|^2+\frac{\lambda}{4}\left|\chi_1^{(1)}\right|^2\right]\eta_1^{(1)}=0$$

$$\varepsilon^1:\Omega_1^2=\frac{1}{I}\left[(\beta+\lambda)+4S\sin^2\left(\frac{qd}{2}\right)+4S_h\sin^2\left(\frac{hqd}{2}\right)\right],$$

$$\Omega_2^2=\frac{1}{I}\left[(2\beta+D+\lambda)+4S\sin^2\left(\frac{qd}{2}\right)+4S_h\cos^2\left(\frac{hqd}{2}\right)\right]$$

$$\varepsilon^2:\upsilon_{g1}=\frac{d\left[S\sin(qd)+hS_h\sin(hqd)\right]}{I\Omega_1},\upsilon_{g2}=\frac{d\left[S\sin(qd)+hS_h\sin(hqd)\right]}{I\Omega_2}$$

$$\varepsilon^3:\left[I-S\left(\frac{d}{\upsilon_{g1}}\right)^2\cos(qd)-S_h\left(\frac{hd}{\upsilon_{g1}}\right)^2\cos(hqd)\right]\frac{\partial^2\chi_1^{(1)}}{\partial\tau_1^2}-iS\sin(qd)\left[\chi_1^{(1)}(m-1)\right]$$

$$-iS_h\sin(hqd)\left[\chi_1^{(1)}(m+h)-\chi_1^{(1)}(m-h)\right]-\left[3\left(\frac{\beta}{2}+\frac{\lambda}{24}\right)\left|\chi_1^{(1)}\right|^2+\frac{\lambda}{4}\left|\eta_1^{(1)}\right|^2\right]\chi_1^{(1)}=0$$

$$\left[I-S\left(\frac{d}{\upsilon_{g2}}\right)^2\cos(qd)+S_h\left(\frac{hd}{\upsilon_{g2}}\right)^2\cos(hqd)\right]\frac{\partial^2\eta_1^{(1)}}{\partial\tau_2^2}-iS\sin(qd)\left[\eta_1^{(1)}(m+1)-\eta_1^{(1)}(m-1)\right]$$

$$+iS_h\sin(hqd)\left[\eta_1^{(1)}(m+h)-\eta_1^{(1)}(m-h)\right]-\left[3\left(\frac{\beta}{3}+\frac{D}{6}+\frac{\lambda}{24}\right)\left|\eta_1^{(1)}\right|^2+\frac{\lambda}{4}\left|\chi_1^{(1)}\right|^2\right]\eta_1^{(1)}=0$$

(9).

Equations at order ε³ lead to the following set of coupled equations

$$i(\chi_{m+1}-\chi_{m-1})+iP(\chi_{m+1}-\chi_{m-1})+Q_1\frac{\partial^2\chi m}{\partial\tau_1^2}+\left[\gamma_{11}|\chi_m|^2+\gamma_{12}|\eta_m|^2\right]\chi_m=0 \tag{10}$$

$$i(\eta_{m+1}-\eta_{m-1})+iP(\eta_{m+1}-\eta_{m-1})+Q_2\frac{\partial^2\eta m}{\partial\tau_2^2}+\left[\gamma_{21}|\chi_m|^2+\gamma_{22}|\eta_m|^2\right]\eta_m=0, \tag{11}$$

with

$$P=\frac{S_h\sin(hqd)}{S\sin(qd)},\gamma_{11}=\frac{3}{4S\sin(qd)}\left(\frac{\beta}{2}+\frac{\lambda}{24}\right),$$

$$\gamma_{12}=\gamma_{21}=\frac{\lambda}{4S\sin(qd)},\gamma_{22}=\frac{3}{4S\sin(qd)}\left(\beta+\frac{D}{2}+\frac{\lambda}{8}\right)$$

$$Q_1=\frac{1}{S\sin(qd)}\left[S\left(\frac{d}{\upsilon_{g1}}\right)^2\cos(qd)+S_h\left(\frac{hd}{\upsilon_{g1}}\right)^2\cos(hqd)-I\right]$$

$$Q_2=\frac{1}{S\sin(qd)}\left[S\left(\frac{d}{\upsilon_{g2}}\right)^2\cos(qd)-S_h\left(\frac{hd}{\upsilon_{g2}}\right)^2\cos(hqd)-I\right] \tag{12}$$

The different features of the frequencies Ω_1 and Ω_2 are shown in Figure 1. In Figure 1(a), we have assumed $S_h = 0$. Since the main purpose of this work is to bring out the impact of the helicoidal coupling on the bearing of localized structures, the different features of the dispersion relation are shown in Figure 1(b)-(d). These figures have been plotted for $S_h < (\beta + D)/4$ [panel (b)], $S_h = (\beta + D)/4$ [panel (c)] and $S_h > (\beta + D)/4$ [panel (d)], respectively. The same features have been observed in the framework of the helicoidal spin-like model [5]. In the presence of helicity, the two branches (acoustic and optical) do not lie at constant distance. This can give rise to one or two crossover point. We can also notice that the presence of such crossover points in the spectrum usually signals the appearance of a complex dynamics. A discussion on this is beyond our scope here. For instance, let us fix the value of S_h which gives one crossover point as $S_{h,cr}$.

From relations (5) and (6), the approximate solutions $\varphi_n(t)$ and $\Phi_n(t)$ of Eqs.(4) can be written as

$$\varphi_n(t) = \varepsilon\chi_m(\tau_1)e^{i(qnd-\Omega_1 t)} + \vartheta(\varepsilon^2) \text{ and } \phi_n(t) = \varepsilon\eta_m(\tau_2)e^{i(qnd-\Omega_1 t)} + \vartheta(\varepsilon^2), \tag{13}$$

Where $\chi_m(\tau_1) = \chi_1^{(1)}(m,\tau_1)$ and $\eta_m(\tau_2) = \eta_1^{(1)}(m,\tau_2)$.

Modulational Instability of Coupled Waves in DNA

It is now a well establish fact that nonlinear systems exhibit an instability that leads to self-induced modulation of the steady state due to interplay between the nonlinear and dispersive effects. Focus on the so-called modulational instability (MI) phenomenon is constantly growing because of its importance as a factor giving rise to intrinsic localized modes. It has been in fact demonstrated that MI generates such localized modes in nonlinear lattices provided discreteness effects are taking into consideration [9,11,12]. In the framework of DNA dynamics, soliton formation through MI has been investigated [5,9,13,16,17], which shows the possibility of solitons and localized structures bearing.

Linear stability analysis

The continuous version of the above system is the coupled NLS equations which are known in various systems. We intend to show in this section that it can be used to describe some relevant features of DNA molecules. We use the technique of MI analysis as done in Ref. [5,16] and we bring out the impact of both nonlinear coupling and helicity. For this purpose, we consider the stationary solutions.

$$\chi_m = A\exp\left[i\left(\xi m - \mu_1\tau_1\right)\right] \text{ and } \eta_m = B\exp\left[i\left(\xi m - \mu_2\tau_2\right)\right] \tag{14}$$

which obey the dispersion relations

$$\mu_1^2 = \frac{1}{Q_1}\left[-2\sin(\xi) - 2P\sin(h\xi) + \gamma_{11}|A|^2 + \gamma_{12}|B|^2\right] \tag{15a}$$

$$\mu_2^2 = \frac{1}{Q_2}\left[-2\sin(\xi) - 2P\sin(h\xi) + \gamma_{21}|A|^2 + \gamma_{22}|B|^2\right] \tag{15b}$$

We solve the above set of equations for $|A|^2$ and $|B|^2$ and get the following system

$$\mu_1^2\left(\gamma_{22}Q_1 - \gamma_{12}Q_2\frac{\mu_2^2}{\mu_1^2}\right) = -\left[2(\gamma_{22}-\gamma_{12})\sin(\xi) + 2P(\gamma_{22}+\gamma_{12})\sin(h\xi) + \left(\gamma_{11}\gamma_{22}-\gamma_{12}^2\right)|A^2|\right] \tag{16a}$$

$$\mu_2^2\left(\gamma_{11}Q_2\frac{\mu_1^2}{\mu_2^2} - \gamma_{12}Q_1\right) = -\left[2(\gamma_{11}-\gamma_{12})\sin(\xi) - 2P(\gamma_{11}+\gamma_{12})\sin(h\xi) + \left(\gamma_{11}\gamma_{22}-\gamma_{12}^2\right)|B|^2\right] \tag{16b}$$

From Eq. (16), wave instabilities will develop in the model under our study if μ_1^2 and μ_2^2 are negative. This means that $\frac{\mu_2^2}{\mu_1^2}$ and $\frac{\mu_1^2}{\mu_2^2}$ are positive. For that reason, we can set $\frac{\mu_2^2}{\mu_1^2} = \frac{\mu_1^2}{\mu_2^2} = 1$. The remaining terms are easy to manage, i.e.,

$$\mu_1^2 = -\frac{1}{\gamma_{22}Q_1 - \gamma_{12}Q_2}\left[2(\gamma_{22}-\gamma_{12})\sin(\xi) + 2P(\gamma_{22}+\gamma_{12})\sin(h\xi) - \left(\gamma_{11}\gamma_{22}-\gamma_{12}^2\right)|A|^2\right] \tag{17a}$$

$$\mu_2^2 = -\frac{1}{\gamma_{11}Q_2 - \gamma_{12}Q_1}\left[2(\gamma_{11}-\gamma_{12})\sin(\xi) - 2P(\gamma_{11}+\gamma_{12})\sin(h\xi) - \left(\gamma_{11}\gamma_{22}-\gamma_{12}^2\right)|B|^2\right] \tag{17b}$$

Modulated waves are then expected in the DNA model under study if the right-hand sides of Eqs. (17) are negative. In this frame, there is no real solutions μ_1 and μ_2 if

$$\gamma_{22}Q_1 - \gamma_{12}Q_2 > 0, |A|^2 > \frac{1}{\gamma_{11}\gamma_{22}-\gamma_{12}^2}\left[2(\gamma_{22}-\gamma_{12})\sin(\xi) + 2P(\gamma_{22}+\gamma_{12})\sin(h\xi)\right] = A_{cr}^2 \tag{18a}$$

$$\gamma_{11}Q_2 - \gamma_{12}Q_1 > 0, |B|^2 > \frac{1}{\gamma_{11}\gamma_{22}-\gamma_{12}^2}\left[2(\gamma_{11}-\gamma_{12})\sin(\xi) - 2P(\gamma_{11}+\gamma_{12})\sin(h\xi)\right] = B_{cr}^2 \tag{18b}$$

On the other hand, if $\gamma_{22}Q_1 - \gamma_{12}Q_2 < 0$ and $\gamma_{11}Q_2 - \gamma_{12}Q_1 < 0$, the plane wave solutions will be unstable if

$$|A|^2 > |A_{cr}|^2 \text{ and } |B|^2 > |B_{cr}|^2 \tag{19}$$

The above equations represent the conditions for plane waves to be unstable in the coupled modified sG equations. In what follows we discuss the impact of the helicoidal coupling on the coupled instability criteria. In this purpose, the following behaviors have been observed:

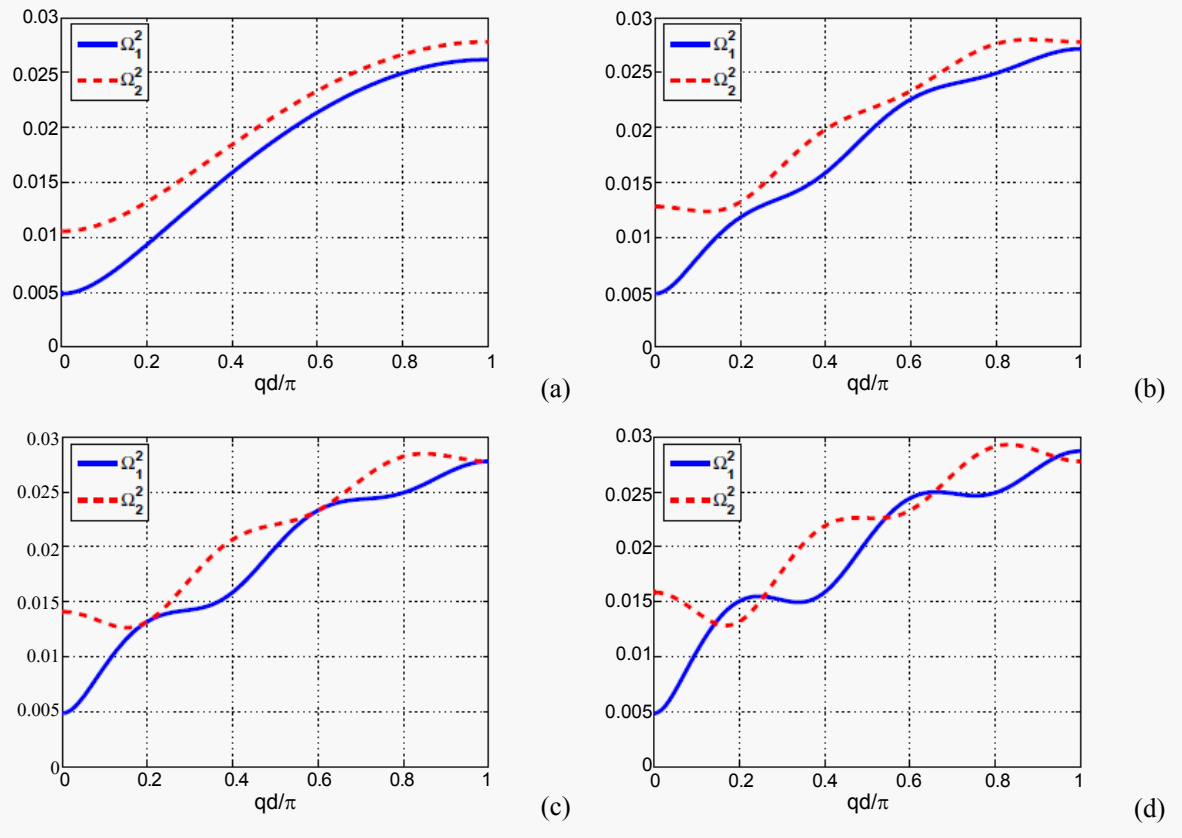

Figure 1: Optical and acoustic frequencies as a function qd and for different values of S_h and S = 0.3 eV, D = 1.2×10^{-1} eV, I = 1.8158×10^{3}Å^2 amu, λ = 4×10^{-3} eV: Panel (a) shows the dispersion curves for S_h = 0. The curves are similar to those obtained for the discrete sG model. For $S_h < S_{h;cr}$, we have the configuration of panel (b). The dispersion curves oscillate and there is no crossing point between the optical and the acoustic curves. When $S_h = S_{h;cr}$, there is one crossing point. Panel (d) shows the dispersion curves for $S > S_{h;cr}$. In this case, there are two crossing points between the optical and the acoustic curves.

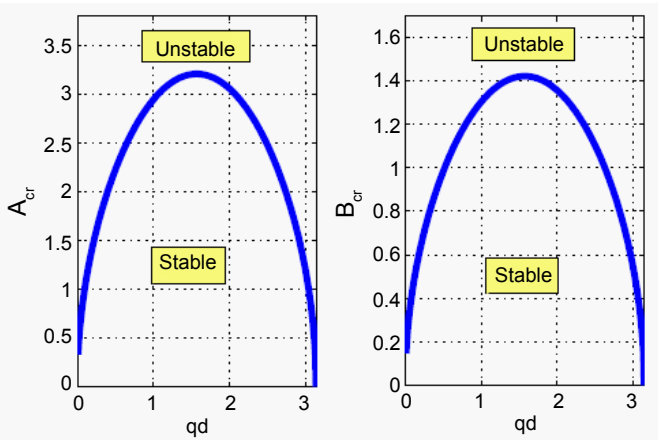

Figure 2: The panel shows the plots the threshold amplitudes A_{cr} and B_{cr} when helicity is not taken into account, with $Q = \pi/2$. Values of parameters are S = 0.3 eV, D = 1.2 × 10^{-1} eV, I = 1.8158 × 10^3 Å.

• For $S_h = 0$, there is no helicoidal coupling and the highest amplitudes of waves will be possible if $\sin(\xi) = 1$, i.e., $\xi = \pi/2$ [15]. The corresponding threshold amplitudes are plotted in Figure 2(a). The system is modulational unstable for $qd \in [0; \pi]$. We see that both equations shear the same parameter values. However, the threshold amplitude A_{cr} is higher than the threshold amplitude B_{cr}.

• For $S_h \neq 0$, the two equations do not shear the same parameter values. The threshold amplitude for the in-phase dynamics will be maximum if $\xi = \pi/2$, while the threshold amplitude for the out of- phase dynamics will be high for $\xi = 3\pi/10$ [5]. This also means that localized structures cannot

be observed for both modes at the same time. Helicity therefore introduces a switching between the unzipping of the molecule and the opening of the base pairs. The molecule first unzips for the hydrogen bonds to be broken. It is also observed that helicity breaks the instability domains into side bands, while in the case $S_h = 0$ there is only one side band. The in-phase dynamics is expected to undergo large oscillations as predicted by Figure 2 (b).

According to the above analysis, it is obvious that in the coupled mode, coupled waves cannot be highly localized at the same time. The in-phase and out-of-phase motions are therefore expected to display different dynamical features as further reinforced by Figure 4, where the critical amplitudes have been plotted versus the helicoidal coupling constant S_h.

Numerical analysis

In previous section, our results are based on the theory of linear stability analysis. However, we know that the linear stability analysis is limited because it can only predict the onset of instability and does not tell us anything about the long-time dynamical behavior of the system when the instability grows [11,12]. To further confirm that our linear instability analysis given above can correctly describe the initial stage of instability in the DNA chain, we exactly solve the set of coupled sG equations Eq.(4) by numerical fourth order Runge-Kutta algorithm. The numerical simulation cannot only confirm our analytical prediction for short time but it can also give the longtime dynamics of the nonlinear DNA system. Periodic boundary conditions have been used and the initial condition has been chosen as to satisfy the combined solutions (13) and (14) (the resulting expression is a modulated wave). In our simulations, when we chose the appropriate values for qd and ξ, we observe the feature of wave breaking displayed by Figure 5. In fact, we bring out the switching of soliton-like structures in the DNA model under our study and confirm that bending and base pair opening cannot occur at the same time. In Figure 5 (a1), the bending of the molecule displays extended soliton-like waves as already observed by Tabi et al. [6], while the strand oscillation plane waves are stable under modulation [see Figure 5 (b1)]. This confirms the accuracy

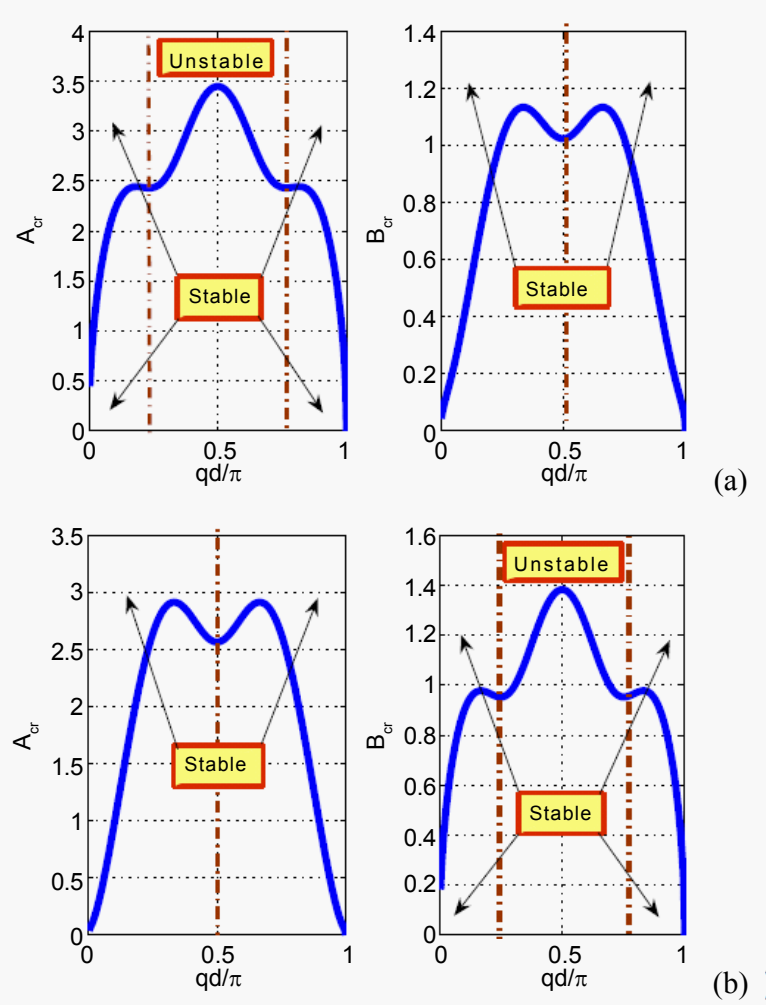

Figure 3: The panels show the features of threshold amplitudes A_{cr} and B_{cr} in the coupled mode when helicity is included. In panel (a) we have plotted the amplitudes for $\xi = \pi/2$ and the panel (b) has been plotted for $\xi = 3\pi/10$. Values of parameters are S = 0.3 eV, $D = 1.2 \times 10^{-1}$ eV, $I = 1.8158 \times 103$ Å^2 amu, $\lambda = 4 \times 10^{-3}$ eV, and h = 5. Arrows point further regions of stability.

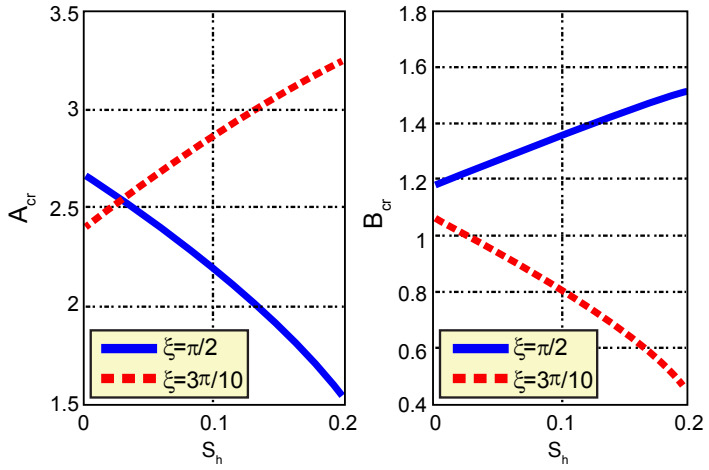

Figure 4: The panels show plots of the threshold amplitudes A_{cr} (first panel) and B_{cr} (second panel) versus the helicoidal coupling constant S_h. Values of parameters have been chosen as S = 0.3 eV, D = 1.2×10^{-1} eV, I = 1.8158×10^3 Å^2 amu.

λ = 4×10^{-3} eV, h = 5, $\xi = \pi/2$ (solid blue line), $\xi = 3\pi/10$ (red dashed line), and $qd = \pi/4$

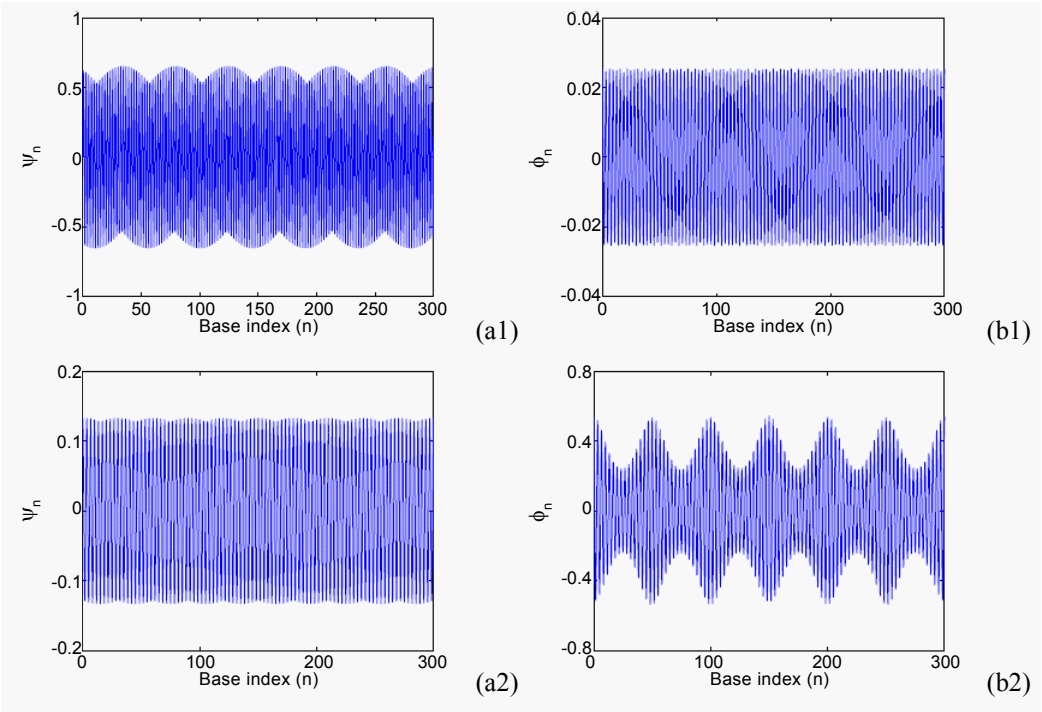

Figure 5: The panels show how the initial plane solution wave breaks into wave train which has the shape of soliton-like objects in the present DNA model, as predicted by the analytical investigations, for ϵ = 0.01, f = 1.5, S = 0.3 eV, D = 1.2×10^{-1} eV, I = 1.8158 × 103 Å^2 amu, λ = 4 × 10^{-3} eV, h = 5, t = 800, and: (a1)-(b1) $\xi = 0.45\pi$, $qd = 0.58\pi$; (a2)-(b2) $\xi = 0.36\pi$, $qd = 0.58\pi$.

of our linear stability analysis performed in the previous section and shows that any process that could take place in the DNA double chain is in close relationship with solitonic structures. Furthermore, the mechanism by which RNA polymerase opens locally the DNA double helix to initiate the transcription is not known, but there is experimental evidence that it involves a bending of the double helix [18,19] before the breaking of the hydrogen bonds linking bases in pairs. Although it cannot claim to describe accurately the actual effect of the bending of a three-dimensional helix, the two-component model can bring insight into this mechanism as already predicted by the linear stability analysis. Using a simple mechanical model of the double helix, it is easy to observe the effects of a local bend: (i) Bases inside the bend are brought closer to each other while the ones which are outside increase their relative distance and finally displays the features observed in Figure 5 (b2), while the bending is stopped for a while.

(ii) This stands for a local unwinding of the helix which occurs in the middle of the bent region while the two regions next to the bend on both sides are on the contrary slightly more twisted. This is due to the rigidity of the two strands entangled in the double helix. That is why we still observe slight oscillations of the bending coefficient which account for the effect of base opening on the whole lattice [see Figure 5 (a2)]. It also accounts for the constant effect of enzymes on the DNA molecule, because, once the genetic code is copied, the messenger-RNA polymerase is always ready to pursue its journey by surfing the long DNA molecule. It is therefore known that local openings of the DNA double helix involve 20 base pairs which are copied in order for the proteins to be synthesized.

Conclusion

The main purpose of the present paper was to introduce the helicoidal coupling in a two-component helicoidal model of DNA, and to bring out the effectiveness of wave switching between the bending of the molecule and the opening of the base pairs. The separation of the strands and the bending of the molecule have been shown to be fully described by a set of coupled sG equations. We have applied the multiple scale expansion to the corresponding set of sG equations, for the first time, and we have shown that the dynamics of the molecule can be described by a set of coupled NLS equations. The linear stability analysis of the latter has shown that when helicity is considered, wave switching was possible. This has been confirmed through the numerical integration of the coupled sG equations which displayed extended waves for the bending and breather-like structures for the oscillations of the hydrogen bond.

Acknowledgements

CBT acknowledges the invitation of the Condensed Matter and Statistical Physics Section (CMSPS) of the Abdus Salam International Centre for Theoretical Physics (ICTP), during which this work was finalized.

References

1. Englander SW, Kallenbach NR, Heeger AJ, Krumhansl JA, Litwin S (1980) Nature of the open state in long polynucleotide double helices. Proc Natl Acad Sci U S A **77:** 7222-7226.
2. Yomosa S (1984) Solitary excitations in deoxyribonuclei acid (DNA) double helices. Phys Rev A 30: 474-480.
3. Takeno S, Homma S (1983) Topological solitons and modulated structure of bases in DNA double helices, Prog Theor Phys 70: 308-311; Homma S, Takeno S (1984) A coupled base-rotator model for structure and dynamics of DNA. Prog Theor Phys 72: 679.
4. Zhang CT (1987) Soliton excitations in deoxyribonucleic acid (DNA) double helices. Phys Rev A 35: 886-891.
5. Tabi CB, Mohamadou A, Kofané TC (2009) Discrete instability in the DNA double helix. Chaos 19: 043101.
6. Tabi CB, Mohamadou A, Kofané TC (2008) Wave propagation of nonlinear modes and formation of bubble in a two-component helicoidal lattice. Eur Phys J D 50: 307-316.
7. Daniel M, Vasumathi V (2009) Solitonlike base pair opening in a helicoidal DNA: An analogy with a helimagnet and a cholesteric liquid crystal. Phys Rev E Stat Nonlin Soft Matter Phys 79: 012901.
8. Dauxois T (1991) Dynamics of breather modes in a nonlinear “helicoidal” model of DNA. Phys Lett A 159: 390-395.
9. Tabi CB, Mohamadou A, Kofané TC (2008) Formation of localized structures in the Peyrard-Bishop-Dauxois model, J Phys Condens Matter 20: 415104.
10. Zdravkovi`c S, Satari`c MV (2007) High amplitude mode and DNA opening. Europhys Lett 78: 38004.
11. Daumont I, Dauxois T, Peyrard M (1997) Modulational instability: first step towards energy localization in nonlinear lattices. Nonlinearity 10: 617.
12. Kivshar YS, Peyrard M (1992) Modulational instabilities in discrete lattices. Phys Rev A 46: 3198-3205.
13. Tabi CB, Mohamadou A, Kofané TC (2009) Modulated Waves in the DNA Double Helix with Finite Stacking Enthalpy Interaction. J Bionanosci 3: 110-117.
14. Leon J, Manna M (1999) Multiscale analysis of discrete nonlinear evolution equations. J Phys A: Math Gen 32: 2845.
15. Leon J, Manna M (1999) Discrete Instability in Nonlinear Lattices. Phys Rev Lett 83: 2324-2327.
16. Tabi CB, Mohamadou A, Kofané TC (2010) Long-range interactions and wave patterns in a DNA Model. Eur Phys J E 32: 327-333.
17. Tabi CB, Mohamadou A, Kofané TC (2010) Modulational instability in the anharmonic Peyrard- Bishop model of DNA. Eur Phys J B 74: 151-158.
18. Heumann H, Richetti M, Werel W (1988) DNA-dependent RNA polymerase of Escherichia coli induces bending or an increased exibility of DNA by specific complex formation. EMBO J **7**: 4379-4381.
19. Schultz SC, Shields GC, Steitz TA (1991) Crystal structure of a CAP-DNA complex: the DNA isbent by 90 degrees. Science 253: 1001-1007.